Supporting Information

One-Step Fabrication of Non-Fluorinated Transparent Super-Repellent Surfaces with Tunable Wettability Functioning Both in Air and Oil

Mengying Long, Shan Peng*, Xiaojun Yang, Wanshun Deng, Ni Wen, Kai Miao, Gongyun Chen, Xinrui Miao and Wenli Deng*

College of Materials Science and Engineering, South China University of Technology, Wushan Road, Tianhe District, Guangzhou 510640, PR China

E-mail: pengshan5213@163.com.
E-mail: wldeng@scut.edu.cn. Tel.: (+86)020-22236708.

Figure S1. Side-view optical image of blue water droplets spherically positioned on TSS.

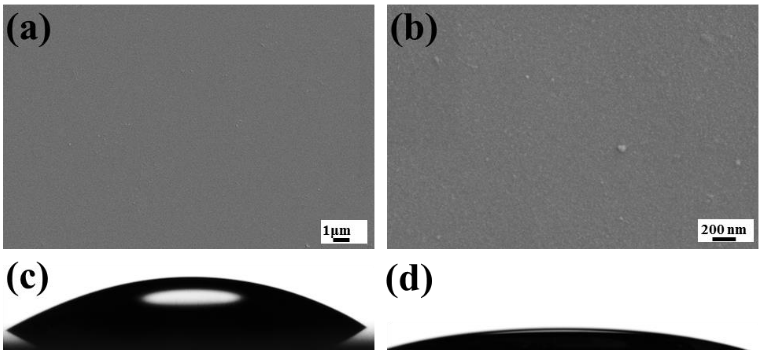

Figure S2. (a, b) Low- and high-magnification SEM images of the original glass slide. (c, d) The shapes of water and ethylene glycol CAs on the original glass slide.

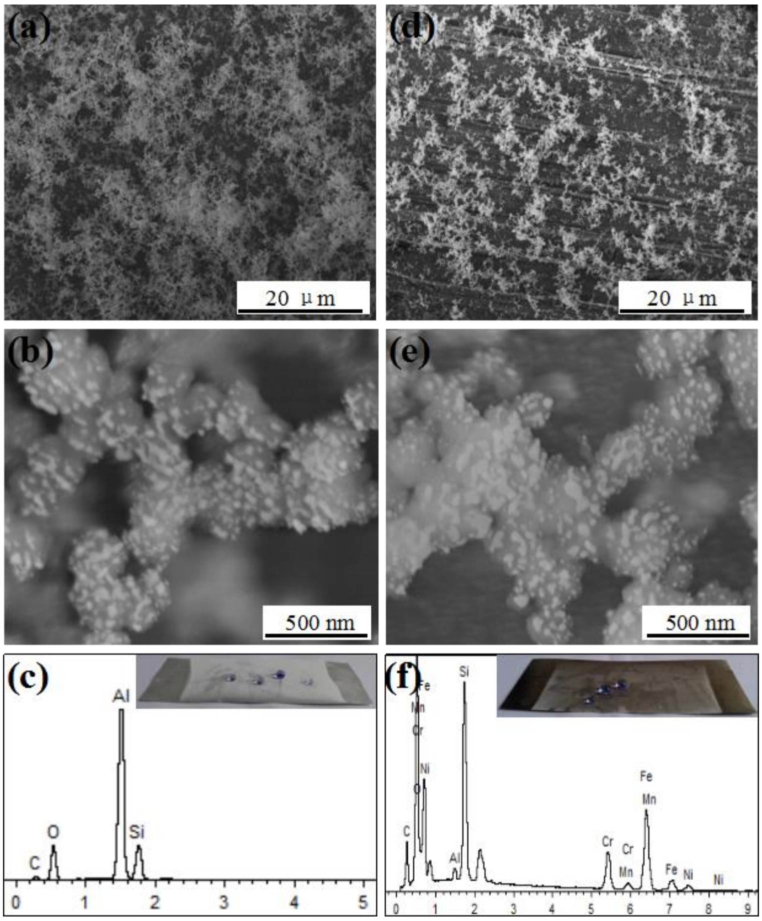

Figure S3. Low- and high-magnification SEM images of (a, d) aluminum and (b, e) steel surfaces after deposition of PDMS soot. (c, f) The EDS spectra of aluminum and steel surfaces after deposition of PDMS soot, and the insets are the blue water droplets positioned on each surfaces.

Aluminum and steel were also treated by the one-step heated with PDMS liquid at 350 ℃ for 2 h, then PDMS soot was successfully adhered on those surfaces. As shown in the SEM images, the hierarchical dual-scale networks are appeared on both surfaces. Si element can be used to track PDMS soot because it contains Si element. From Figure S3c and f, Si element exists on aluminum and steel surfaces, demonstrating that PDMS soot is successfully deposited on the surfaces. Blue water droplets keep spherical on the prepared aluminum and steel surfaces (the inset images of Figure S3c and f), which prove superhydrophobicity of both surfaces. Therefore, rough structure and low surface energy substance are successfully obtained at the same time on aluminum and steel substrates.

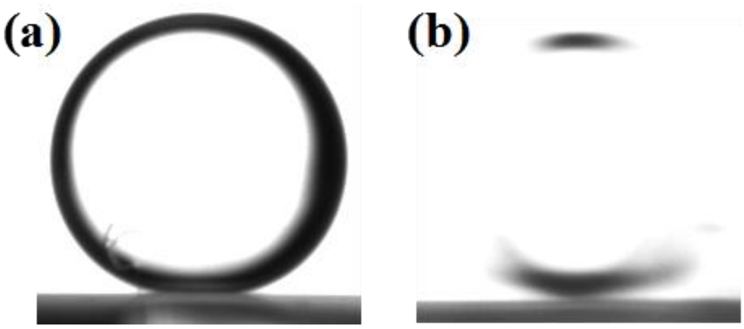

Figure S4. The water CA and SA shapes of TSS in petroleum ether.

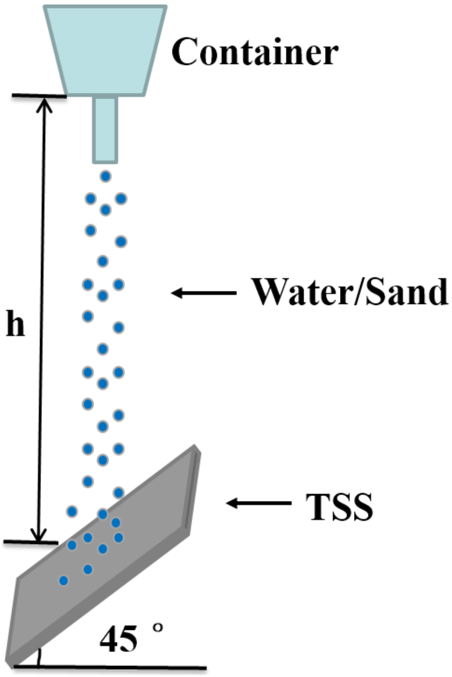

Figure S5. Schematic drawing of water- or sand-flow impacts experiments.

Figure S6. Self-cleaning behaviors of the TSS in petroleum ether after 10 months storage.

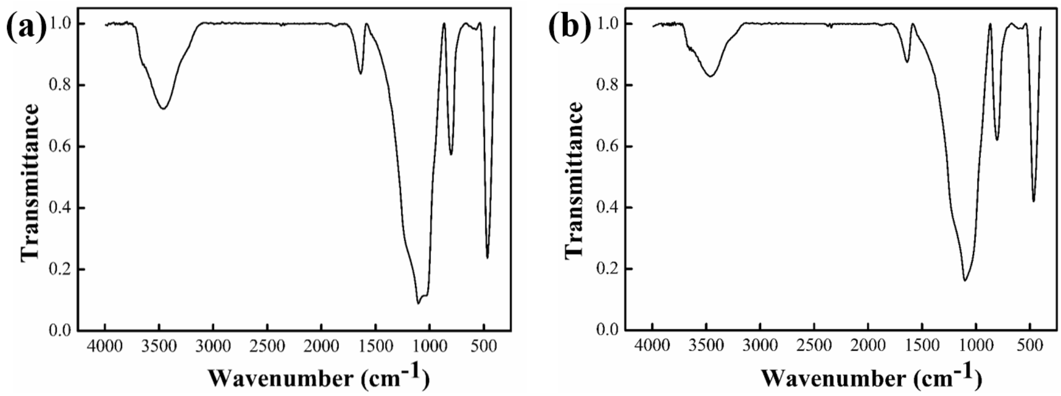

Figure S7. FT-IR spectra of the PDMS-soot-deposited glass slides at (a) 500 ℃, (b) 550 ℃ for 2 h.

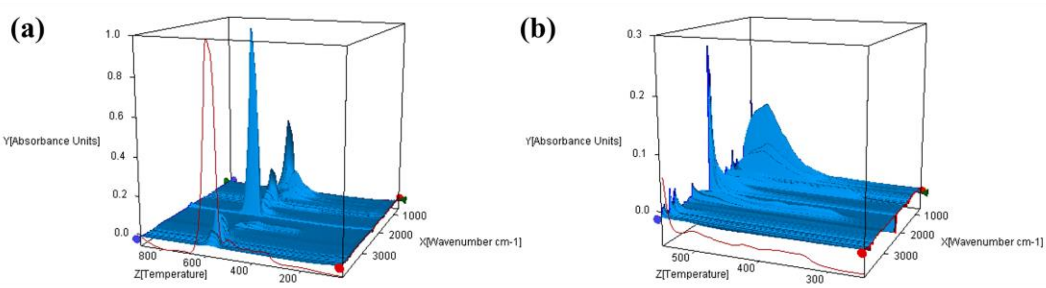

Figure S8. 3D TG/FT-IR diagrams of PDMS pyrolysis gas products at the temperatures in the range of (a) 25–900 ℃ and (b) 250–550 ℃.

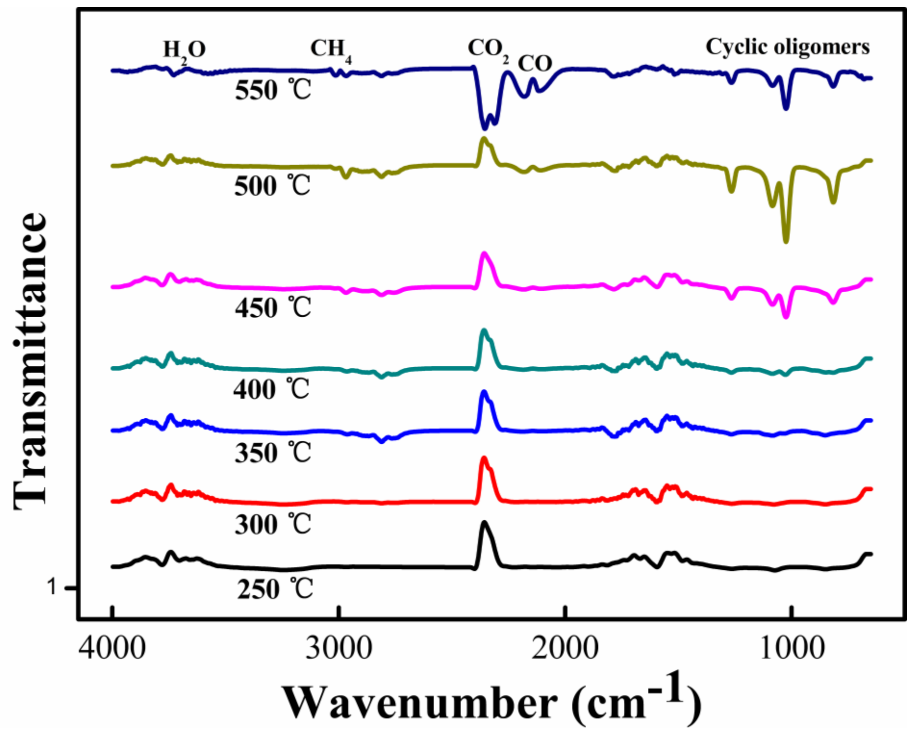

Figure S9. FT-IR spectra of pyrolysis products for PDMS liquid at different temperature. It is clearly seen that the cyclic oligomers (2814 cm^{-1}, 1267 cm^{-1}, 1090 cm^{-1} and 814 cm^{-1}), CO (2114 cm^{-1}), CO_2 (2355 cm^{-1}, 2303 cm^{-1}), CH_4 (3014 cm^{-1}), and H_2O (3500–3700 cm^{-1}) compose of the pyrolysis products at 550 ℃.

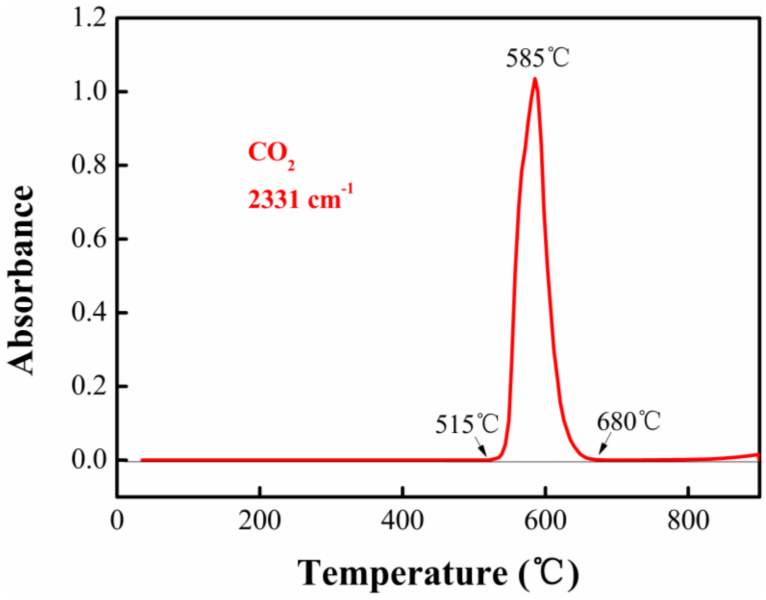

Figure S10. The relationship between temperature and FT-IR absorbance of CO_2 at 1020 cm^{-1}.

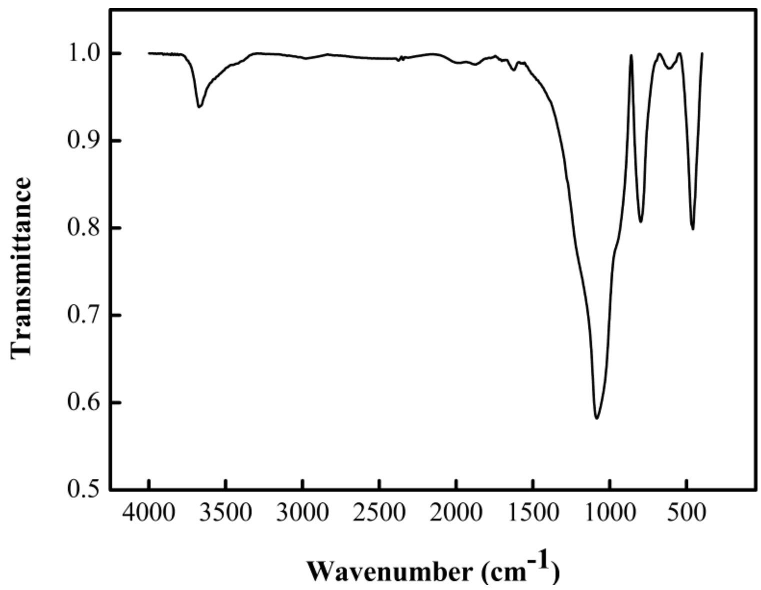

Figure S11. FT-IR spectra of the residual powder at 400 ℃ for 2 h.